EARTHQUAKE ENGINEERING AND STRUCTURAL DYNAMICS
Earthquake Engng. Struct. Dyn. **28**, 501–528 (1999)

ESTIMATION OF INELASTIC DEFORMATION DEMANDS IN MULTISTOREY RC FRAME BUILDINGS

T. B. PANAGIOTAKOS AND M. N. FARDIS*
Department of Civil Engineering, University of Patras, P.O. Box 1424, 26500 Patras, Greece

SUMMARY

Estimation of peak inelastic deformation demands is a key component of any displacement-based procedure for earthquake-resistant design of new structures or for seismic evaluation of existing structures. On the basis of the results of over a thousand non-linear dynamic analyses, rules are developed for the estimation of mean and upper-characteristic peak inelastic interstorey drifts and member chord rotations in multistorey RC frame buildings, either bare or infilled in all storeys but the first. For bare frame structures, mean inelastic deformation demands can be estimated from a linear, equivalent static, or preferably multimodal response spectrum analysis with 5 per cent damping and with the RC members considered with their secant stiffness at yielding. 95 per cent characteristic values can be estimated as multiples of the mean deformations. For open-first-storey buildings, the linear analysis can be equivalent static, with the infills modelled as rigid bidiagonal struts and all RC members considered with their secant stiffness to yielding. Copyright © 1999 John Wiley & Sons, Ltd.

KEY WORDS: displacement-based design; inelastic dynamic analysis; inelastic seismic response; multistorey buildings; open-ground-storey buildings; RC frame buildings

1. INTRODUCTION

Structural displacements and member deformations do not enjoy a primary role in current force-based earthquake-resistant design. Their absolute magnitude is of interest only for aspects considered of secondary importance for seismic performance and safety: for the limitation of non-structural damage, through the control of interstorey drifts, for the calculation of P–Δ effects, for the control of pounding between adjacent structures, etc. In the main phase of current force-based design, namely that of member proportioning for given strength demands and of member detailing, structural displacements and member deformations enter in an average sense and indirectly, through their ratio to the corresponding value at yield (i.e. through the displacement ductility ratio, global or local, which determines, respectively, the force reduction factor or the member detailing requirements). Recent years have seen, however, an increased interest in the

*Correspondence to: M. N. Fardis, Department of Civil Engineering, University of Patras, P.O. Box 1424, University Campus, GR 26500 Patras, Greece. E-mail: mnf@pat.forthnet.gr

Contract/grant sponsor: European Commission; Contract/grant numbers: ENV4-CT97-0548 (DG12-ESCY), FMRX-CT96-0022 (DG12-RSRF)

CCC 0098–8847/99/050501–28$17·50

Received 4 September 1998
Revised 12 November 1998

absolute magnitude of peak displacements and deformation demands. The main reason for this is the recent recognition that displacement- and deformation-, rather than strength-, demands and capacities, is what determines seismic performance and safety. Moreover, ductility factors, although convenient for the determination of strength demands, are poor descriptors of deformation capacity, as the introduction of another, sometimes ill-defined variable, i.e. the yield displacement or deformation, often increases rather than reduces the uncertainty. Recent displacement-based proposals for seismic design of new[1–8], or for the evaluation of existing structures[9–11], define the seismic input in terms of displacement demands. They also use, directly or indirectly, member deformations for the proportioning and detailing of new members or for the evaluation of existing ones. Implementation of these new proposals requires development of procedures for simple, yet relatively accurate, estimation of inelastic displacement and deformation demands throughout the structure.

Previous work on inelastic displacement demands has focused mainly on SDOF systems.[1,12–14] It has essentially confirmed the validity of the equal displacement approximation for systems with natural period T greater than the 'predominant period' of the site or of the ground motion, T_c, i.e. the corner period at which the elastic acceleration and pseudovelocity response spectra both exhibit a local maximum. For $T < T_c$ inelastic displacement demands exceed the elastic. The shorter the period T and the lower the yield strength of the SDOF system, the larger is the peak inelastic displacement of such a short-period system relative to the elastic value.[14] On the contrary, if T_c is clearly predominant in the motion, as, e.g. in records on soft soil, the equal displacement approximation overestimates inelastic displacement demands in the vicinity of T_c.[12,13,15,16]

According to several recent proposals,[15–17] in multistorey buildings inelastic demands for interstorey drifts and other important local deformation measures are estimated through multistage procedures. In these procedures an equivalent SDOF system is first established, its inelastic displacement demands are estimated as in SDOF systems[1,12–14] and are translated then into local deformation demands, either through multiplicative conversion factors derived from a large number of non-linear analyses of representative types of structural systems,[15–17] or through building- and member-specific relationships between global displacements and local deformations, developed through an incremental non-linear static ('pushover') analysis of the building.[15]

The recent NEHRP guidelines for the seismic evaluation and retrofit of existing buildings[11] accept various levels of analysis of increasing complexity for the estimation of inelastic deformation demands in 'deformation-controlled' (i.e. ductile) regions of the building: 'linear static', under equivalent lateral forces with a heightwise distribution simulating first-mode response; 'linear dynamic', i.e. multimodal response spectrum analysis; 'non-linear static', or 'pushover' analysis, with two different heightwise distributions of lateral forces; and 'non-linear dynamic', i.e. inelastic time-historey analysis. In the first three types of analyses the equal displacement approximation is adopted for $T > T_c$, while for $T < T_c$ a multiplicative factor is applied to elastic displacements, which is a function of T and of the expected level of non-linearity. For buildings in which more than 30 per cent of the base shear capacity is provided by elements which degrade under cyclic loads (e.g. 'ordinary' moment frames with no special provisions for local and global ductility, or shear-critical walls), the so-estimated displacement demands are increased to account for the effect of degradation and pinching of the hysteresis loops on inelastic energy dissipation.[11] A further semi-empirical amplification of displacements for P–Δ effects is typically relevant only for very flexible structures. Finally, the rehabilitation guidelines developed in parallel by ATC specifically for RC buildings,[18] advocate estimation of local and global inelastic deformation

demands by combining a Composite Spectrum (which determines the force and displacement demands as a function of the global displacement ductility factor) with a 'pushover' analysis (which determines the global force–displacement relationship up to ultimate). This, in principle, iterative technique accounts for the effects of period lengthening and energy dissipation on inelastic seismic demands, as such effects are reflected by the Composite Spectrum. However, unlike the 'linear dynamic' and the 'non-linear dynamic' procedures of the NEHRP guidelines,[11] it does not capture higher mode effects.

In References 3, 6, 9, global forces and displacements are also related as in the Composite Spectrum approach, i.e. through the secant stiffness to peak displacement and the ductility-dependent damping ratio. A displacement profile is postulated, depending on the structural configuration and the likely or desired plastic mechanism. This is done only to relate the ultimate deformation in critical regions to the equivalent displacement of the SDOF system and not for apportioning global displacement demands to individual members.

In this paper results of several hundreds of non-linear dynamic analyses are utilized for the development of procedures for the estimation of member inelastic deformation demands in bare or partially infilled multistorey RC buildings. In an effort to stay close to everyday earthquake-resistant design practice, the proposed procedures are linear elastic, equivalent static or multi-modal dynamic. The appeal of the proposed approach is reduced, though, by the fact that, similar to non-linear analysis procedures, it requires knowledge of member longitudinal reinforcement. The reason is that member elastic rigidities are computed from yield moments and deformations. For existing buildings this is not a problem, if as-built drawings are available. For new buildings, though, application of the proposed procedures requires preliminary proportioning of member longitudinal reinforcement, for the ultimate-limit-state against factored gravity loads, for damage control under a serviceability earthquake and to meet capacity-design requirements.[7,8] This complication of the computational procedure seems, though, unavoidable, because estimation of inelastic displacement and deformation demands in RC structures is much more sensitive to the elastic rigidities of cracked members than to the details and sophistication of the analysis and the modelling. Moreover, it is now widely recognized that the elastic stiffness of cracked RC members is approximately proportional to yield strength and hence is not a function of cross-sectional dimensions alone, but of the quantity of longitudinal reinforcement as well.[6]

2. DESCRIPTION OF THE RC FRAME BUILDINGS

2.1. Bare frame structures

Rules for the estimation of inelastic deformation demands are derived from analyses of the three types of RC frame buildings shown in Figure 1. Four versions of each building type are considered, which differ in their seismic design parameters: in two of them the design PGA is $0{\cdot}15\,g$ and in the other two it is $0{\cdot}3g$. All of them are designed according to Eurocode 8, Parts 1–1 to 1–3,[19] which provides for three 'Ductility Classes' (DC): High (H), Medium (M) and Low (L), with corresponding behaviour factors q (i.e. force reduction factors R) equal to 5·0, 3·75 and 2·5, respectively. Member detailing becomes less stringent as the DC and the value of q decrease, and so do capacity design requirements: in DC L no capacity design rule applies, in DC M capacity design in shear is required only for columns, while the overstrength factors for capacity design of columns in bending and in shear are higher in DC H than in DC M.

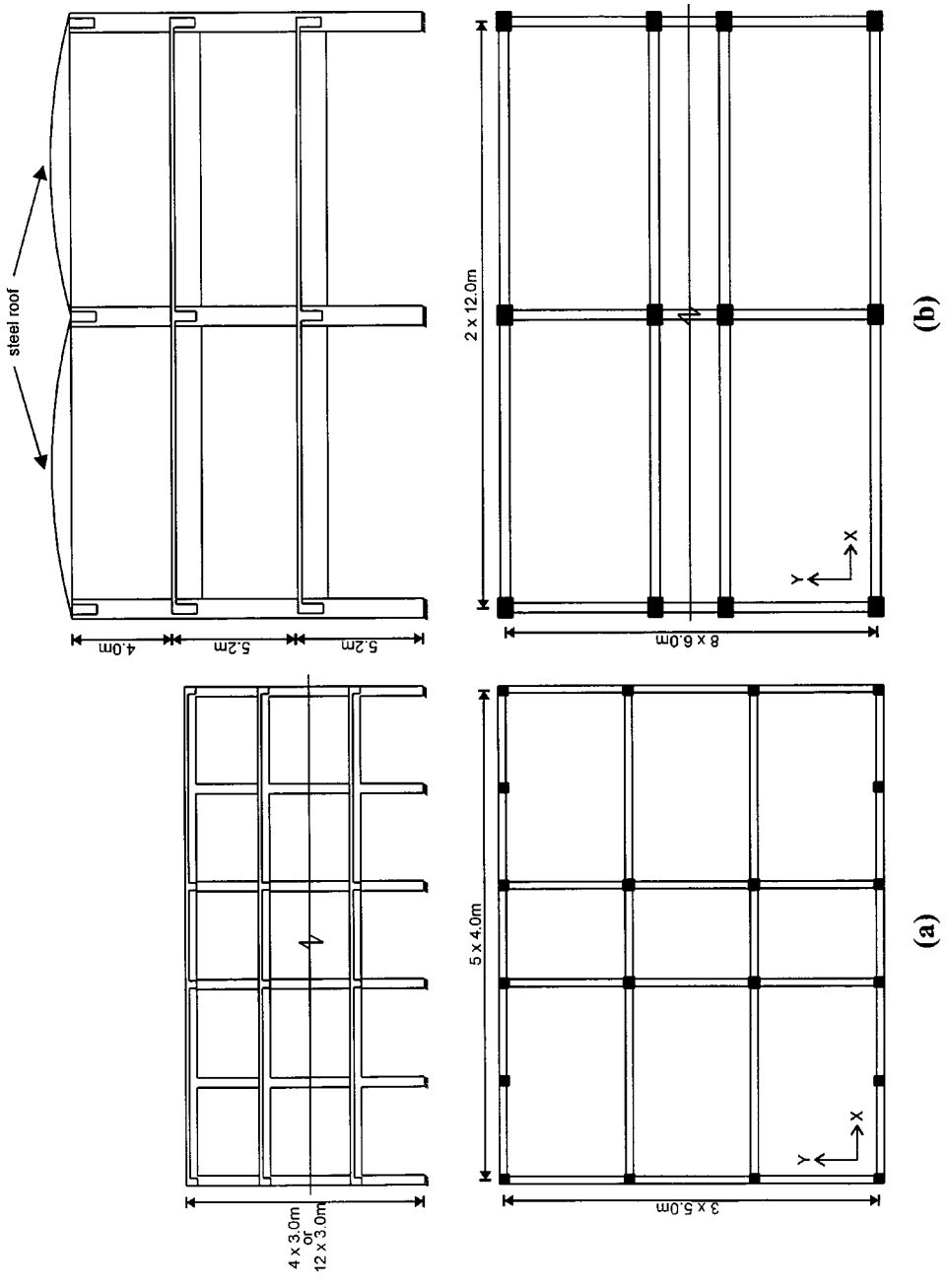

Figure 1. Plane and vertical section of buildings: (a) four-storey and 12-storey buildings; (b) three-storey buildings

The Eurocode 8 acceleration design spectrum for Soil B (intermediate) is used. It falls linearly from the PGA to a value of $2{\cdot}5 \times \mathrm{PGA}/q$ at $T_c/4$, remains flat up to the corner period T_c ($= 0{\cdot}6$ for Soil B) and falls thereafter as $T^{-2/3}$. A multimodal response spectrum analysis was applied for the design. Following Eurocode 8, the design spectrum was entered with periods computed on the basis of gross uncracked sections.

Member cross-sectional dimensions for the four designs (denoted L15, M15, M30 and H30) in each type of building are listed in Table I. They are the same in all storeys, resulting in a very regular configuration, not only in plan but also in elevation (with the exception of the three-storey buildings, in which the top storey differs significantly from the lower two). Except for the application of minimum reinforcement provisions, member reinforcement was proportioned exactly to meet the requirements from the analyses.

To consider the effect of the beam–column strength ratio on the response, versions M15, M30 and H30, which are subject to column capacity design, are designed either with conventional full capacity design (i.e. enforcing $\sum M_{\mathrm{Rc}} > \gamma \sum M_{\mathrm{Rb}}$ at beam–column joints, with subscript b: beams and c: columns, M_{R} = flexural capacity and γ equal to 1.2 for DC M or 1.35 for DC H), or to the relaxed capacity design allowed by Eurocode 8 (i.e. with $\sum M_{\mathrm{Rc}} \geqslant (1 + \gamma - \delta)\delta \sum M_{\mathrm{Rb}}$, with $\delta = \sum M_{\mathrm{Sb}} / \sum M_{\mathrm{Rb}}$ and $\sum M_{\mathrm{Sb}}$ denoting the sum of beam seismic moments at the joint according to the analysis). Accordingly, seven different building designs were produced for each structural configuration, i.e. a total of $3 \times 7 = 21$ building designs. Conventional or relaxed capacity design is signaled by adding a C or R, respectively, to the basic designation of the building (e.g. as M15C vs. M15R). Finally, although the contribution of slab reinforcement to the top flange of the beams in tension was neglected in design, in the non-linear analyses two cases are considered for each building design, one with 'zero' participation of the slab to the tension flange, and another with 'full' participation, meaning that all slab bars parallel to the beam and up to a distance equal to one-quarter of the beam span from it or mid-distance to the next beam, are considered fully effective as beam top flange reinforcement. 'Zero' or 'full' slab participation to the beam tension flange is denoted by adding the ending 0 or F, respectively, to the designation of the building design. The 'zero' slab case reflects how the building is considered in design, e.g. during the application of column capacity design. The 'full' slab case, on the contrary, reflects better the as-built reality. The combination of conventional capacity design and 'zero' slab, i.e. cases C0, correspond to the lowest beam–column strength ratio for the same building geometry and seismic design parameters, whereas the RF combination of relaxed capacity design and 'full' slab corresponds to the highest. The storey-average beam–column strength ratio, $\sum M_{\mathrm{Rb}} / \sum M_{\mathrm{Rc}}$, is about 0·3 to 0·5 in the C0 cases of the low-rise buildings or around 0·25 in those of the 12-storey ones. In the RF low-rise buildings the storey-average $\sum M_{\mathrm{Rb}} / \sum M_{\mathrm{Rc}}$ ratio is nearly double (between 0·6 and 1·0) and that of the 12-storey buildings is around 0.35.[20] So finally the seven different designs for each building configuration are translated into 14 different frame structures for the non-linear analyses, i.e. a total of $3 \times 14 = 42$ different RC structures.

2.2. *Open-ground-storey infilled structures*

The relaxed-capacity-design full-slab-participation version of each building (i.e. buildings L15F, M15RF, M30RF and H30RF) is considered with all bays of the external frames in the two horizontal directions X and Y infilled in all storeys except the ground one. The masonry infills are considered to have a cracking strength τ_{cr} of 0·26 MPa, a shear modulus G of 1·25 GPa and an Elastic Modulus of 2·5 and 8·2 GPa in the horizontal and vertical direction, respectively.

Table I. Member cross-sectional dimensions (m) of 12 buildings

No. of storeys	Design		Columns			Beams b/h			Slab thickness
	DC	PGA (g)	Internal	External	Corner	X-dir/Ext†	X-dir/Int†	Y-dir.	
4	L	0·15	0·50 × 0·50	0·45 × 0·45	0·40 × 0·40	0·25/0·45	0·30/0·60	0·25/0·45	0·14
4	M	0·15	0·50 × 0·50	0·45 × 0·45	0·40 × 0·40	0·25/0·45	0·30/0·60	0·25/0·45	0·14
4	M	0·30	0·50 × 0·50	0·45 × 0·45	0·40 × 0·40	0·30/0·50	0·30/0·60	0·30/0·50	0·14
4	H	0·30	0·50 × 0·50	0·45 × 0·45	0·40 × 0·40	0·30/0·50	0·30/0·60	0·30/0·50	0·14
12	L	0·15	0·80 × 0·80	0·70 × 0·70	0·70 × 0·70	0·30 × 0·60	0·30 × 0·60	0·30 × 0·60	0·14
12	M	0·15	0·80 × 0·80	0·70 × 0·70	0·70 × 0·70	0·30 × 0·60	0·30 × 0·60	0·30 × 0·60	0·14
12	M	0·30	0·80 × 0·80	0·70 × 0·70	0·70 × 0·70	0·35 × 0·60	0·35 × 0·60	0·35 × 0·60	0·14
12	H	0·30	0·80 × 0·80	0·70 × 0·70	0·70 × 0·70	0·35 × 0·65	0·35 × 0·65	0·35 × 0·65	0·14
3	L	0·15	0·50 × 0·80	0·50 × 0·60	0·50 × 0·60	0·30/0·80	0·30/0·80	0·40/1·20	0·16
3	M	0·15	0·50 × 0·80	0·50 × 0·60	0·50 × 0·60	0·30/0·80	0·30/0·80	0·40/1·20	0·16
3	M	0·30	0·60 × 1·00	0·60 × 0·80	0·60 × 0·80	#	#	0·40/1·20	0·16
3	H	0·30	0·60 × 1·00	0·60 × 0·80	0·60 × 0·80	#	#	0·40/1·20	0·16

† The two columns for the beams in the X-direction refer to the external and the internal frames in this direction.
# For strength reasons, the cross-sectional dimensions of the X-direction beams need to vary from 0·35/1·00 in the first to 0·30/0·9 in the second and to 0·30/0·80 in the third storey.

Table II. Infill strength in open-ground-storey buildings

No. of storeys	Design	Infill strength/building mass		Infill strength/design base shear	
		Dir. X	Dir. Y	Dir. X	Dir. Y
4	L15	0·17	0·135	1·21	0·94
4	M15	0·17	0·135	1·77	1·38
4	M30	0·17	0·135	0·87	0·68
4	H30	0·17	0·135	1·13	0·89
12	L15	0·045	0·035	0·38	0·31
12	M15	0·045	0·035	0·57	0·46
12	M30	0·045	0·035	0·29	0·22
12	H30	0·045	0·035	0·37	0·29
3	L15	0·11	0·06	0·86	0·42
3	M15	0·11	0·06	1·29	0·62
3	M30	0·11	0·06	0·56	0·32
3	H30	0·11	0·06	0·74	0·42

These properties correspond to measured values on good-quality masonry in running bond, with 0·112 mm thick vertically perforated bricks. They can be considered representative of single-wythe partitions without openings, or of double-wythe external walls with some openings. The total ultimate shear strength of infills in a storey, considered as 1.3 times the corresponding cracking strength, is listed in Table II as a fraction of the total mass of the building (i.e. as equivalent base shear coefficient) and as a multiple of the design base shear of the bare frame. The 12-storey building and the three-storey one in the short (Y) direction can be considered as lightly infilled in the upper storeys, whereas the four-storey building and the three-storey one in the long (X) direction is moderately infilled. The frame strength and stiffness is always enough to confine the infill panels and to control the global seismic response.

The 12 open-ground-storey buildings are considered in three alternative versions: In the first the RC structure is designed as a bare frame, neglecting the weak-storey effect possibly introduced by the partial infilling. In the second, the weak-storey effect is accounted for, by proportioning the ground storey columns and the 1st-floor beams to resist, on top of the design base shear of the bare structure, the full ultimate shear strength of the infills in the overlying storey. This is effected according to Eurocode 8, Part 1–3, Section 2.9, i.e. by multiplying seismic internal forces (moments, shears and axial forces) in these beams and columns from the analysis for the design earthquake, by $1 + \alpha$, where α is the ratio of the infill strength to the design base shear (listed in the last two columns of Table II). If there is no large overstrength in the frame members of the overlying storey, this approach amounts to full capacity design protection of the RC members of the open storey. Finally, in the third alternative this procedure for designing against the weak-storey effects is applied only to the columns of the open ground storey, as large chord rotations at the ends of the first-floor beams are prevented by the large shear stiffness of the infill panels. The first of these three design versions is closer to existing structures, which are normally not designed against the open-storey effects. The third version is closer to a new structure for which the designer provides a reasonable amount of column

overstrength against the weak storey effect. Finally, the second version is a strict application of a current code.

3. NON-LINEAR DYNAMIC RESPONSE ANALYSES

3.1. Introduction

The 42 different bare frame structures and the 36 open-ground-storey infilled ones, are subjected to non-linear dynamic analysis of their response to unidirectional ground motions applied separately in horizontal directions X and Y. The input motions consist of four synthetic

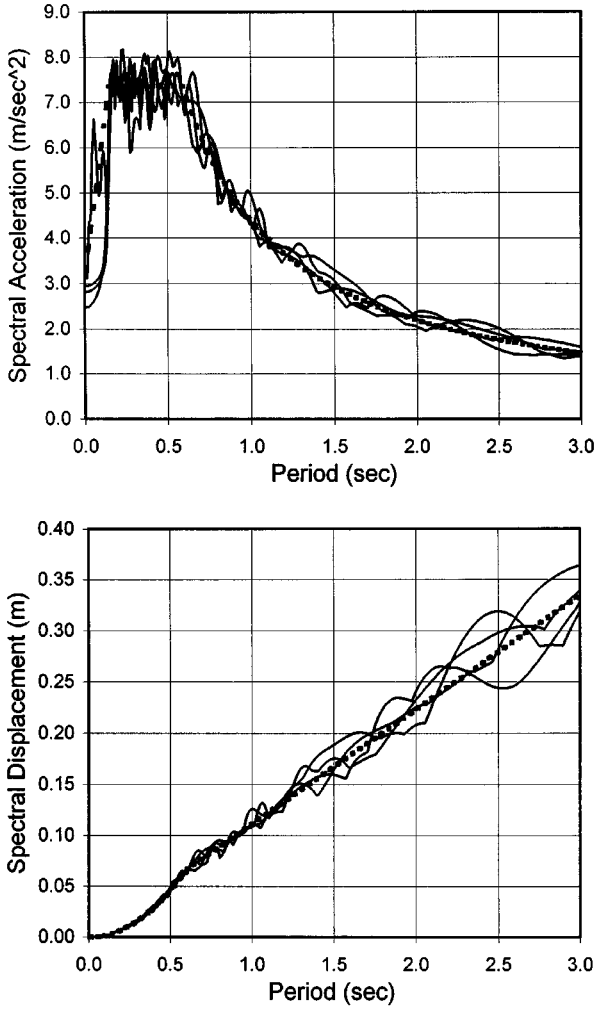

Figure 2. Acceleration and displacement spectra of four synthetic motions and target Eurocode 8 spectra for PGA $= 0{\cdot}3g$

10 sec-long accelerograms, with rise and fall times of 1·5 sec. The motions are compatible to the elastic Eurocode 8 spectrum for soil B, which increases linearly from PGA to 2·5 PGA at $T_c/4$, remains constant up to T_c (= 0·6 sec) and falls then with $1/T$. The elastic acceleration and displacement spectra of the four motions are compared to the target spectra in Figure 2. Their rms (root-mean-square) deviation from the EC8 spectrum within the velocity-controlled period range of 0·6 to 3·0 sec is 7·5 per cent of the corresponding spectral value.

The input motions are applied to the bare frames after scaling to an effective PGA (defined as in ATC and NEHRP documents) of 1·0x, 1·5x or 2·0x the design PGA of 0·15 or 0·3g, and to the open-ground-storey structures after scaling to 1·0x and 2·0x the design PGA. So each bare structure is subjected to $4 \times 3 = 12$ non-linear analyses in each horizontal direction, giving a total of $42 \times 12 \times 2 = 1008$ analyses, and each partially infilled one to $4 \times 2 = 8$ analyses in X or Y, amounting to a total of $36 \times 8 \times 2 = 576$ non-linear analyses.

3.2. *Non-linear modelling*

One-component, point-hinge macromodels are used for the RC members, to relate the end-moment to the chord rotation at member ends within each plane of bending. Inelastic coupling between the two ends of the member is not considered, i.e. the plastic component of the chord rotation at one end is taken independent of the current value and of the history of the moment at the other end. Although coupling between the two ends is considered in the elastic range, the elastic rigidity, EI, and the parameters of the post-yield moment chord rotation relationship are computed assuming that the point of inflection is fixed at element mid-length, i.e. considering antisymmetric bending. Then if M_y is the yield moment at the end-section, computed at first yielding of the tension steel assuming plane sections remain plane, and θ_y is the chord rotation at the same end at yielding, for a shear span equal to half the member length L, then the elastic rigidity EI is computed as $\mathrm{EI} = (M_y/\theta_y)L/6$. The value of θ_y can be estimated as the sum of three components: a flexural one, equal to $\theta_y L/6$ (θ_y is the curvature at yield, computed with the same assumptions as the yield moment M_y), a second one due to shear deformations and inclined cracking along the shear span, and a third one, s/z, due to the pull-out, s, of the tension steel from its anchorage zone beyond the end-section (z is the lever arm of internal forces). Semi-empirical expressions for the shear contribution to θ_y and for the bar slippage, s, have been fitted to test results in References 7, 21 or 22. These expressions provide roughly similar results and can be used almost equivalently for the calculation of θ_y. So, although joints are modelled as rigid zones at member ends, bar slippage in them is included in the member model, albeit in an indirect and crude way.

In beams, each end corresponds to two values of $\mathrm{EI} = (M_y/\theta_y)L/6$, one for positive and another for negative bending. These values are averaged at both ends to provide a single EI-value for the member. For columns with symmetric reinforcement and cross-section, the two single values at each end are averaged; these values are computed on the basis of the column axial force due to the acting gravity loads alone.

The M–θ relation in monotonic loading is taken bilinear, with a post-yield hardening ratio p computed assuming antisymmetric bending and using empirical expressions in References 6, 21 or 23. The ultimate moment M_u is computed on the basis of first principles. The hysteresis rules supplementing the bilinear monotonic M–θ curve are of the modified-Takeda type,[24] with reloading parameter $\beta = 0$ (reloading to the extreme previous point of the monotonic curve) and

with unloading parameter $a = 0{\cdot}3$ (unloading to a residual deformation $(1 - a)$ times that for elastic unloading). This choice of parameters produces hysteretic damping in cycles at a displacement ductility factor μ equivalent to a damping ratio $\zeta = (1 - p)(1 - a)(1 - 1/\mu)/\pi \approx 0{\cdot}22(1 - 1/\mu)$, in addition to the 5 per cent viscous damping considered to be associated with the elastic regime.[26]

P–Δ effects are included, through the linearized geometric stiffness matrix of columns.

In the partially infilled structures infill panels are modelled as bidiagonal struts effective only in compression. Their axial force–deformation law reproduces a phenomenological model fitted to test results on the panel shear stress–shear deformation (i.e. storey drift ratio) relation. In monotonic loading the model is multilinear, with the first corner, τ_{cr}, γ_{cr} at cracking, the second, τ_u, γ_u, at ultimate strength and the third at a residual strength at the end of the post-ultimate falling branch. The ultimate strength, τ_u, is taken equal to $1{\cdot}3\tau_{cr}$, the cracking strain equal to τ_{cr}/G and the strain at ultimate, γ_u, is established considering that the panel secant stiffness of the equivalent strut to ultimate strength can be computed from the equivalent strut width formula in Reference 25 using the elastic modulus of the masonry in the horizontal (weak) direction. These simple rules depend on masonry properties which can be measured on standard wallette tests in diagonal compression (for τ_{cr} and G) and in compression parallel and normal to the bed joints (for E), and have been found[27] to provide good fit to test results on simple infilled frames.

Unloading from the envelope curve is linear at the elastic slope G, down to about 10 per cent of the ultimate strength, τ_u, followed by a more shallow linear unloading–reloading branch up to a point in the opposite direction at a stress level of $\sim 0{\cdot}1\tau_u$, and at a shear strain exceeding the elastic value $0.1\tau_u/G$ by 80 per cent of the maximum previous post-cracking shear strain $(\gamma - \gamma_{cr})$, in the direction of reloading. Further reloading heads to the envelope curve, through a point which is 15 per cent below the most extreme previous point on the envelope. These rules provide good overall fit to cyclic test results. In the first post-cracking cycle they give hysteretic damping equivalent to a viscous damping ratio of 20–30 per cent or of 5–6 per cent in subsequent full cycles.[27]

Viscous damping is of the Rayleigh type,[28] with a modal damping ratio specified equal to 5 per cent at the fundamental elastic period of the cracked structure, T_{cr}, and at half that period.

The modelling approach and assumptions in this study were found to be in satisfactory agreement with cyclic, pseudodynamic or shake table tests on full- or large-scale subassemblies and structures, bare or partially infilled. Further validation was provided through comparisons with non-linear dynamic analyses of configurations L150, M15R0, M30R0 and H30R0 of the 12-storey structure in direction X using a very detailed fibre model for the RC members. Details of the validation can be found in References 20, 29, 30.

Mean values of material strengths are used in the non-linear analyses instead of the corresponding design values. This difference corresponds to an overstrength factor of approximately 1·5. Further overstrengths on the supply side due to minimum reinforcement, the control of some sections by factored gravity loads, the coverage of both beam or column sections on opposite sides of a joint by the same steel bars, the consideration of accidental torsion and of motion multidirectionality (SRSS or 1 : 0·3 combination of the effects of the two horizontal components), etc., increase the value of the overstrength factor to more than 2·0. Overstrength is further increased to an aggregate value of 2·5–3·0, because calculation of natural periods on the basis of gross uncracked sections leads to significant overestimation of seismic design forces.

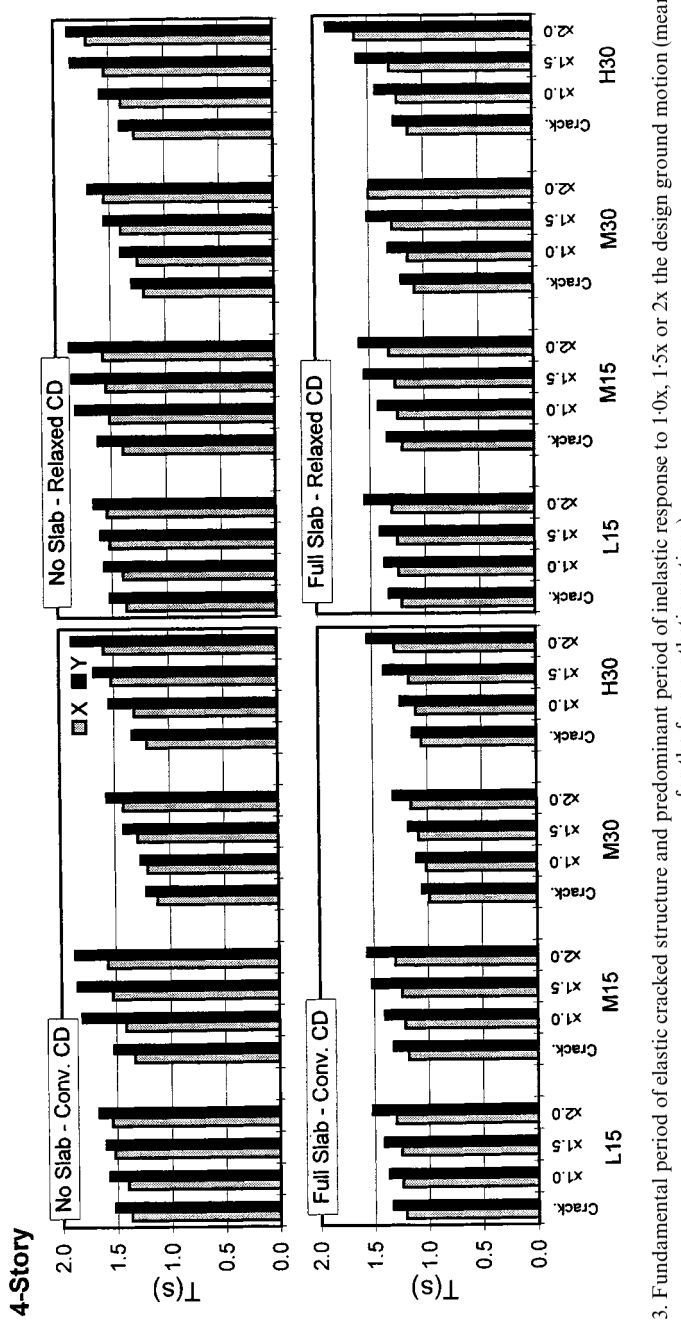

Figure 3. Fundamental period of elastic cracked structure and predominant period of inelastic response to 1·0x, 1·5x or 2x the design ground motion (mean values for the four synthetic motions)

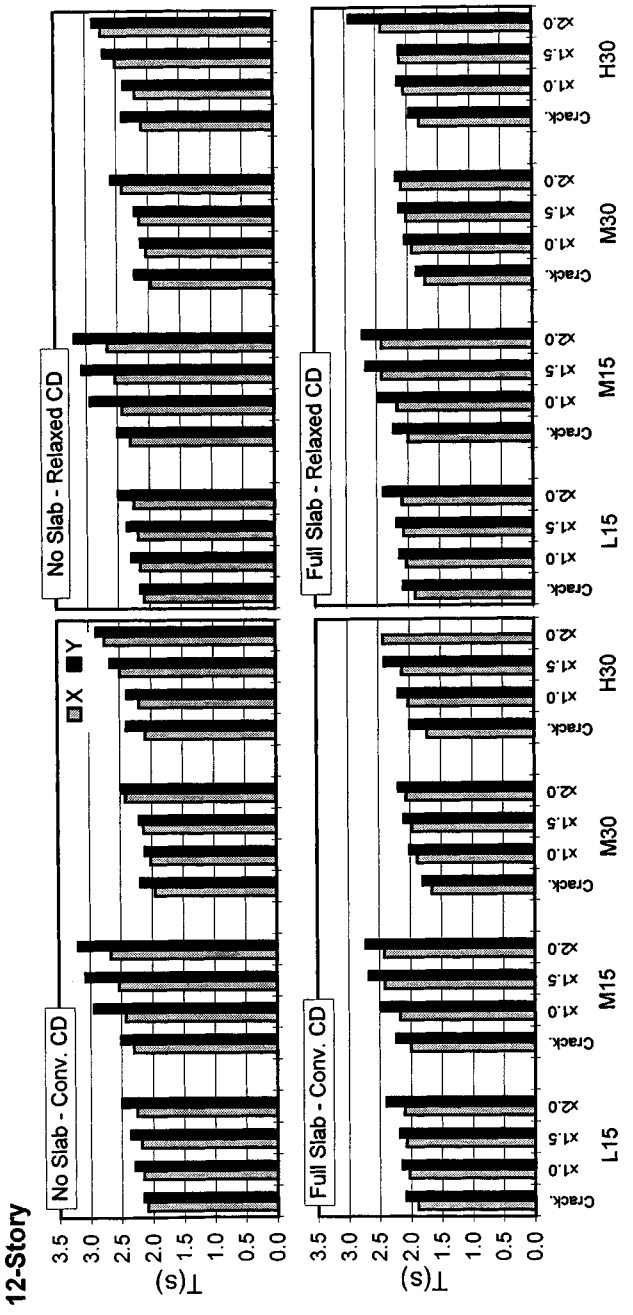

Figure 3. (*Continued*)

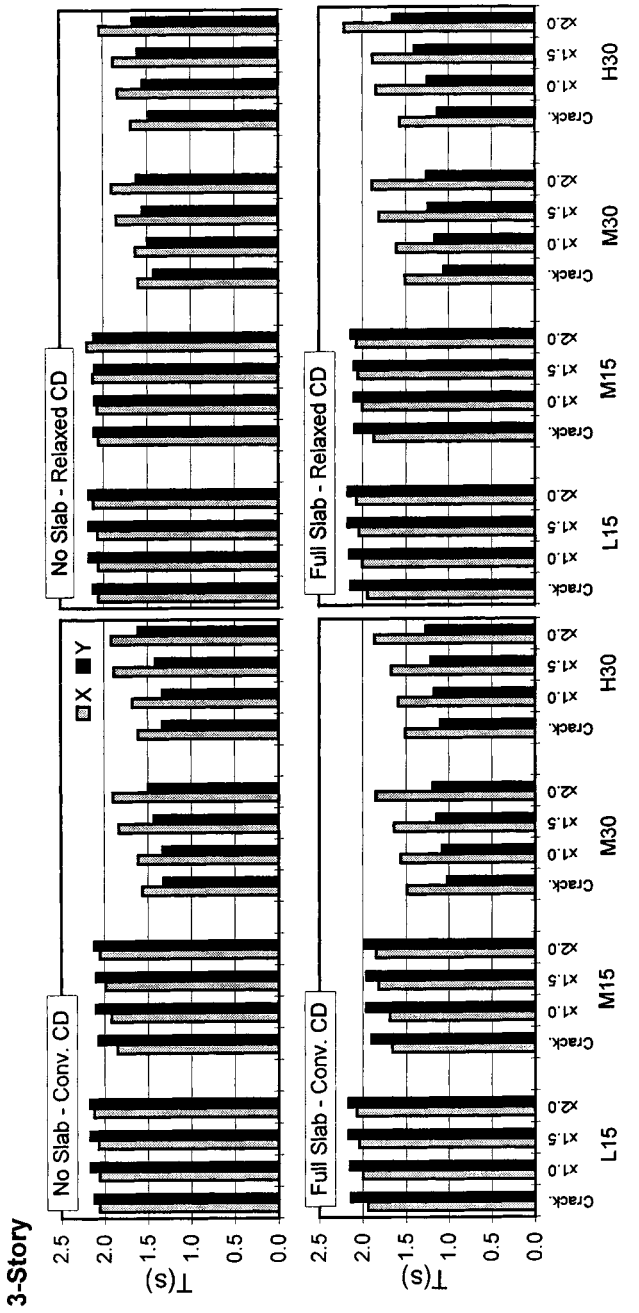

Figure 3. *(Continued)*

3.3. Predominant period of non-linear response

The predominant period of the non-linear displacement response, T_{nl}, has been determined from a Fourier analysis of the calculated top displacement time-history. Its (average over the 4 input motions) value at the three excitation levels, 1·0x, 1·5x and 2·0x, is presented in Figure 3 for the bare structures in the form of bar-charts and compared to the fundamental period of the elastic structure, T_{cr}. As expected T_{nl} always exceeds T_{cr}, but not very much, and increases with the level of excitation. Both T_{cr} and T_{nl} are significantly affected and in the same direction by the type of capacity design (C or R) and by the slab width included in the beam tension flange in the analysis (0 or F). It is interesting to note that the values of T_{cr} are well above the corner period T_c of the excitation and that the values of T_{cr} and T_{nl} range over the entire velocity-controlled part of the spectrum, in which the 'equal displacement rule' applies well on the average for SDOF systems.

In an effort to be on the conservative side as far as the acceleration and force demands are concerned, the rules of current force-based seismic design codes for the calculation of the fundamental elastic period of RC structures on the basis of gross uncracked sections (through eigenvalue analysis or the Rayleigh quotient) underpredict these periods by almost a factor of 2·0. Full-scale pseudodynamic or shake table tests and sophisticated models alike, show that the fundamental period of even low-rise bare RC structures, under motions which cause full cracking of the concrete and bring several members to incipient yielding, is normally longer than the predominant or corner period T_c of the excitation. This increases the magnitude and the importance of seismic displacements, but facilitates their estimation on the basis of the equal displacement rule.

3.4. Inelastic deformation demands of bare structures

The deformation measures of interest here are the chord rotations at member ends and the interstorey drift ratios. Computed chord rotations reflect, in part, the effects of bond slippage within beam column joints and are the most useful deformation measure for evaluation of the deformation capacity of a member or for its detailed design to meet the seismic deformation demands. Interstorey drift ratios are equal to the sum of the average chord rotation of the beams and the average chord rotation of the columns in the storey (plus the average shear strain in beam–column joints, which is neglected though in the present analyses). They are not directly useful for member evaluation or proportioning, but they provide a good picture of the distribution of inelastic deformation demands among the storeys.

Computed inelastic interstorey drift ratios and chord rotations at member ends are presented in the form of ratios to the corresponding deformation measures from a linear elastic analysis of the structure. Two types of elastic analyses are considered: Equivalent static under storey lateral forces proportional to the product of mass and elevation (inverted triangular distribution), or multimodal response spectrum analysis, with the CQC rule for combination of peak modal responses.[30] Both types of analysis use the 5 per cent-damped smooth elastic spectrum of Eurocode 8 for Soil B, from which the four synthetic motions were generated. They both use the same elastic rigidities $EI = (M_y/\theta_y)L/6$ for the members as the non-linear analyses.

A detailed examination of the results shows that within each class of buildings with the same number of storeys, differences in the member dimensions and reinforcement and in the

beam–column strength ratio are not statistically important. In other words, the differences between cases L15, M15, M30 and H30, and between cases C and R or 0 and F affect similarly the elastic global and the inelastic deformation demands and their distribution in the structure. This conclusion extends to the two different horizontal directions (which correspond to two different structural configurations) and to the three intensities of the input motion (implying that the distribution of inelasticity within the structure does not change much with motion intensity). Examples of this insensitivity are shown later in Figures 7 and 8. For this reason inelastic-to-elastic ratios for interstorey drifts are lumped together in a single database with 336 data points for each type of building (4-, 12- or 3-storey) and presented in Figure 4, separately for each method of elastic analysis. The scatter represented by the standard deviation and by the difference between the mean and the 95 per cent-characteristic values in Figure 4 reflect variability due to the above-mentioned differences in the structural configuration and the member dimensions and reinforcement, and due to the intensity and the details of the input motion. According to Figure 4, the multimodal response spectrum elastic analysis provides better overall agreement in the mean (esp. in the top third of the building, see, in particular, the slightly irregular three-storey case) and smaller dispersion than the equivalent static procedure.

Figure 5 refers to member chord rotations, shown separately for beams and columns of each floor. For the ground-storey columns, results are shown separately for the connection to the foundation at 'gr' and for the top, at floor '1'. For the other floors no distinction is made in Figure 5 between top and bottom of columns. The mean $\pm$ one standard deviation range reflects now in addition, the member-to-member variability within each storey (there are 20 different column ends in each storey of the 4- or 12-storey structures or 36 in the three-storey ones and there are 16 different beam ends in X or 12 in Y in the first two types of structures or 32 and 20, respectively, in the third). Accordingly the dispersion, expressed by the standard deviation and by the difference between the mean and the 95 per cent-characteristic values, is now larger than for the interstorey drifts. The mean value is also larger, however, especially when the elastic analysis is equivalent static. The reason seems to be that for given interstorey drift ratio the non-linear analysis produces more balanced chord rotations at the two ends of the same member, whereas the elastic analysis and especially the equivalent static, gives larger imbalances between the two ends, which are translated at the end, due to effect of the division by the smaller of the two end chord rotations, to a bias of the mean towards values greater than 1·0. This effect has been also observed in Reference 31. The multimodal response spectrum analysis gives again overall better agreement in the mean, smaller dispersion and lower 95 per cent-characteristic values than the equivalent lateral force procedure, especially for beams. Finally, mean and upper-characteristic values of the inelastic-to-elastic chord rotation ratio are, on the average, lower in columns than in beams, especially when the elastic analysis is of the multimodal response spectrum type. This may imply that, although capacity design of columns and, in general, the low beam-to-column strength ratio do not limit inelasticity and plastic hinge formation to the beams alone,[20,28] the inelastic chord rotation demands in columns are still smaller than in beams and hence they are better predicted by an elastic analysis, especially a multimodal one.

Table III summarizes the results in Figures 4 and 5, in terms of the heightwise variation and the building average of the mean and of the 95 per cent-characteristic inelastic-to-elastic deformation ratio. The values listed at the base and roof levels provide good linear fit to the storey values in Figures 4 and 5 and can be used for linear interpolations. It is encouraging that the large scatter and the large deviations of the mean and of the 95 per cent-characteristic values from 1·0 take place in the upper storeys, which are less critical, as the absolute magnitude of inelastic

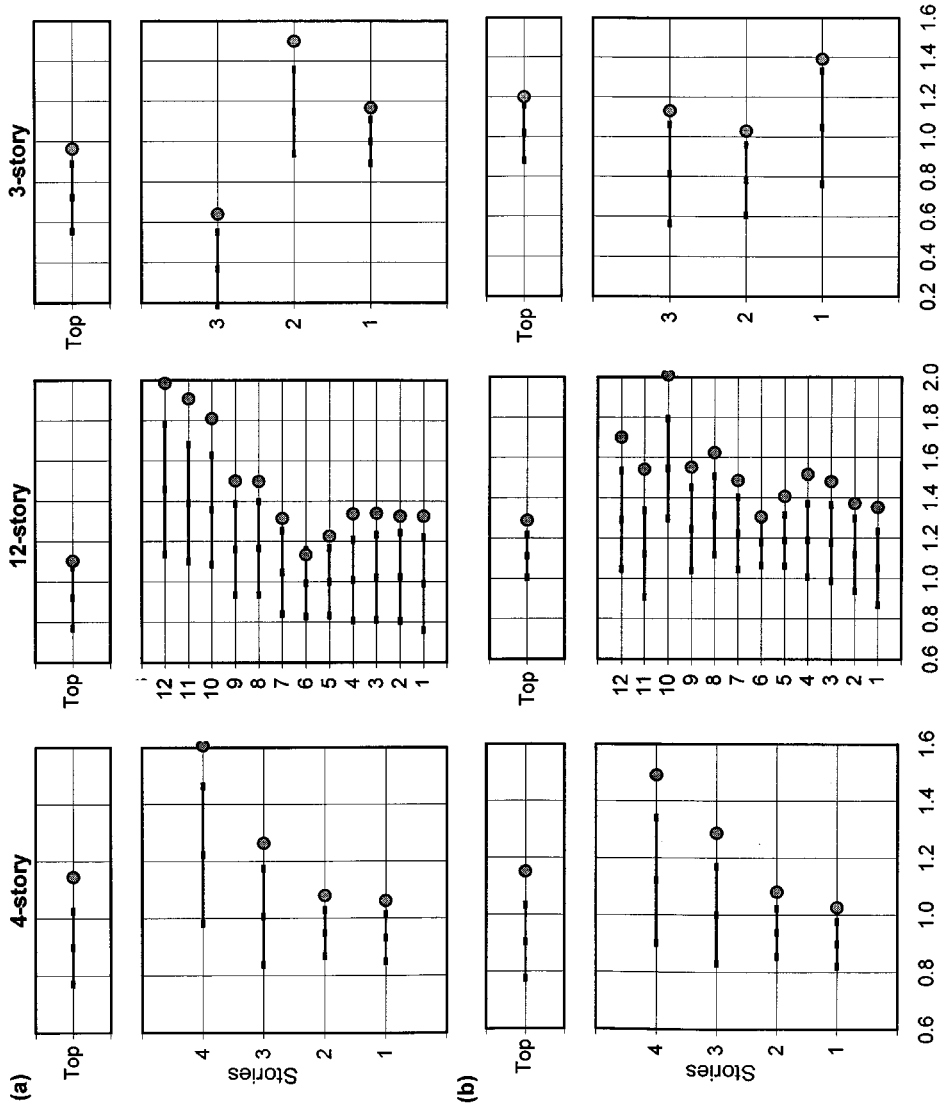

Figure 4. Mean ± standard deviation range and 95 per cent-characteristic value of inelastic-to-elastic interstorey and top drifts (horizontal axis), for elastic drifts computed from: (a) static analysis with equivalent lateral loads; (b) multimodal response spectrum analysis

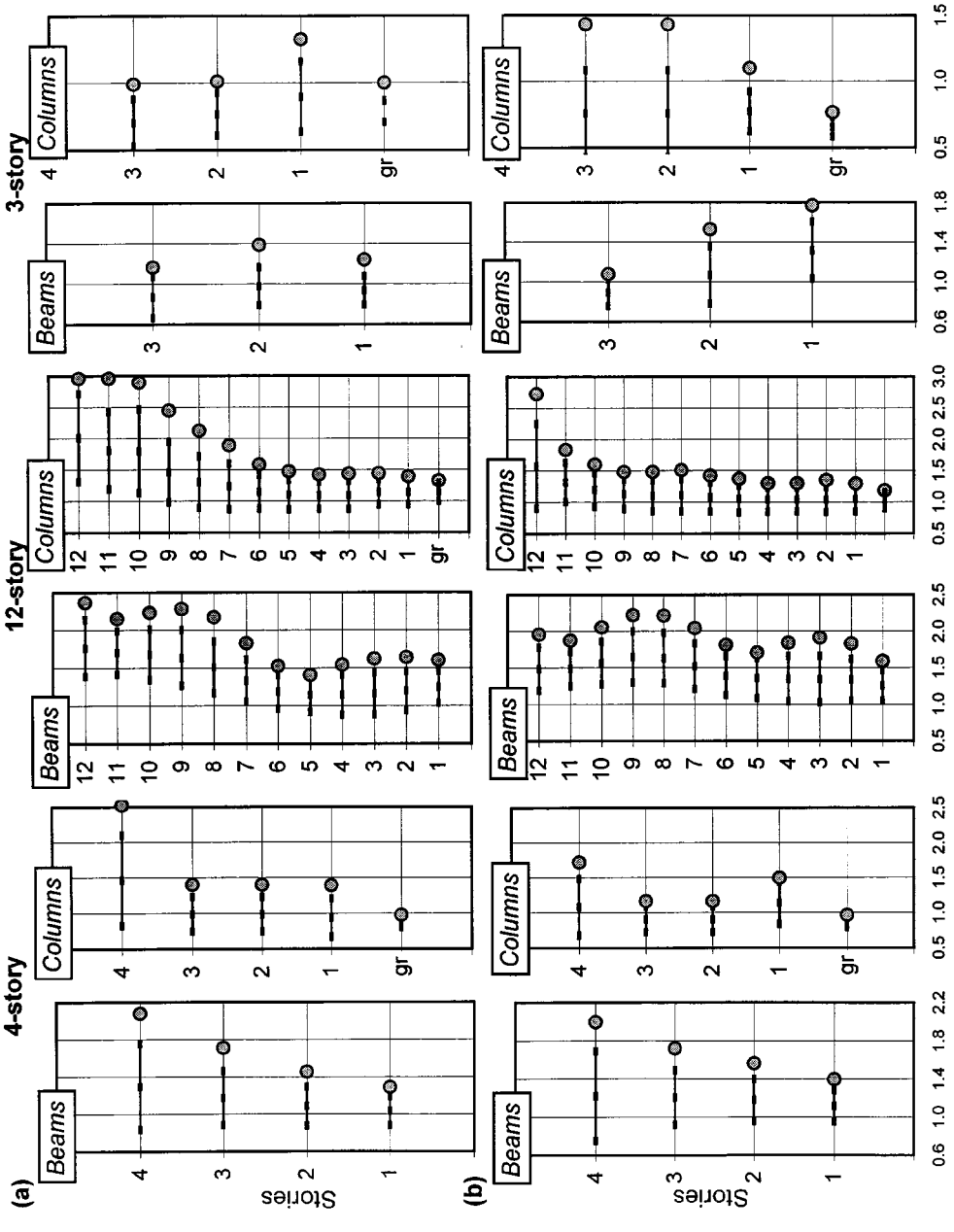

Figure 5. Mean ± standard deviation range and 95 per cent-characteristic value of inelastic-to-elastic chord-rotation (horizontal axis), for elastic chord rotations computed from: (a) static analysis with equivalent lateral loads; (b) multimodal response spectrum analysis

Table III. Heightwise variation and building average of inelastic-to-elastic interstorey drift or chord rotation ratio (mean and 95 per cent-characteristic values)

No. of storeys		Interstorey drift				Beam chord rotation				Column chord rotation			
		Mean		95 per cent-char.		Mean		95 per cent-char.		Mean		95 per cent-char.	
		Stat.	Dyn.	Stat.	Dyn.	Stat.	Dyn.	Stat.	Dyn.	Stat.	Dyn.	Stat.	Dyn.
4	Roof	1·15	1·1	1·45	1·4	1·25	1·2	2·0	1·95	1·15	1·0	2·0	1·55
	Base	0·9	0·9	1·0	1·0	1·0	1·1	1·3	1·4	0·85	0·85	1·0	0·95
	Avg.	0·99	1·01	1·24	1·17	1·12	1·15	1·64	1·67	0·99	0·93	1·51	1·24
12	Roof	1·25	1·35	1·75	1·7	1·6	1·6	2·25	2·15	1·6	1·2	2·65	1·75
	Base	1·0	1·05	1·25	1·35	1·1	1·2	1·5	1·7	1·0	1·0	1·25	1·3
	Avg.	1·13	1·20	1·45	1·51	1·35	1·41	1·87	1·93	1·30	1·09	1·96	1·53
3	Roof	0·6	0·8	0·8	1·0	0·8	0·9	1·2	1·05	0·75	0·85	1·05	1·65
	Base	1·2	1·0	1·3	1·3	0·9	1·3	1·3	1·8	0·9	0·65	1·1	0·9
	Avg.	0·87	0·91	1·10	1·12	0·85	1·11	1·26	1·42	0·82	0·74	1·07	1·29
All	Roof	1·0	1·1	1·35	1·35	1·2	1·25	1·85	1·7	1·15	1·0	1·9	1·65
	Base	1·05	1·0	1·2	1·2	1·0	1·2	1·35	1·65	0·9	0·85	1·1	1·05
	Avg.	1·00	1·05	1·26	1·27	1·11	1·22	1·59	1·67	1·04	0·92	1·51	1·35

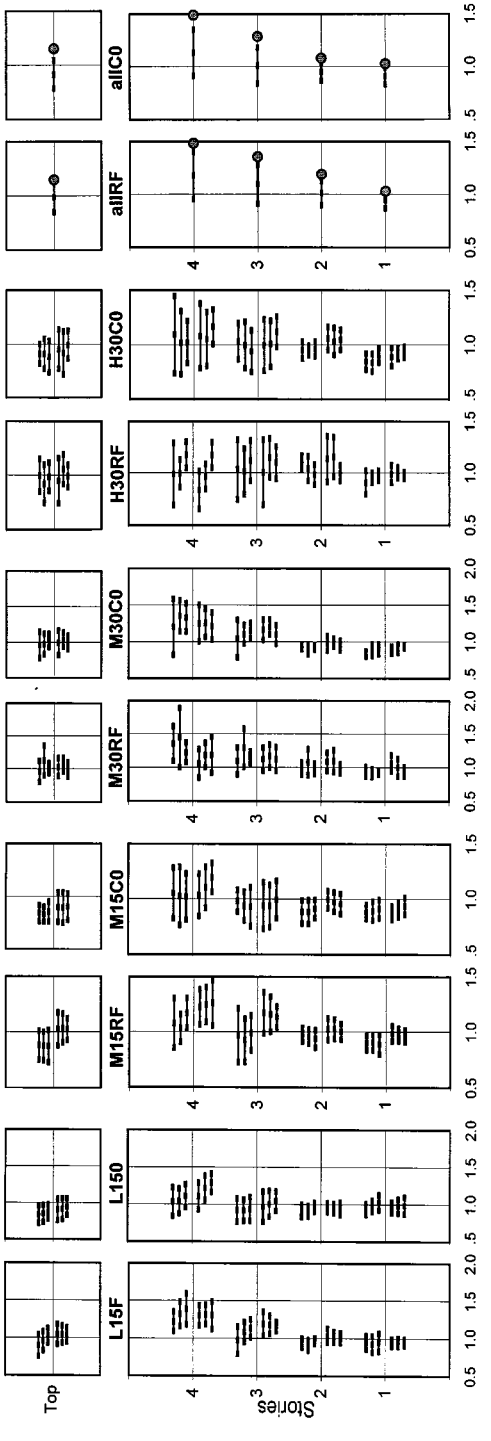

Figure 6. Mean ± standard deviation range of inelastic-to-elastic ratio of interstorey and top drifts in individual four-storey buildings, with 'full' (F) or 'zero' (0) slab participation to beam tension flange and with conventional (C) or relaxed (R) column capacity design. (Upper three or lower three ranges: *X* or *Y* direction. Top or bottom range in the triplet: design motion x2 or x1; intermediate: x1·5)

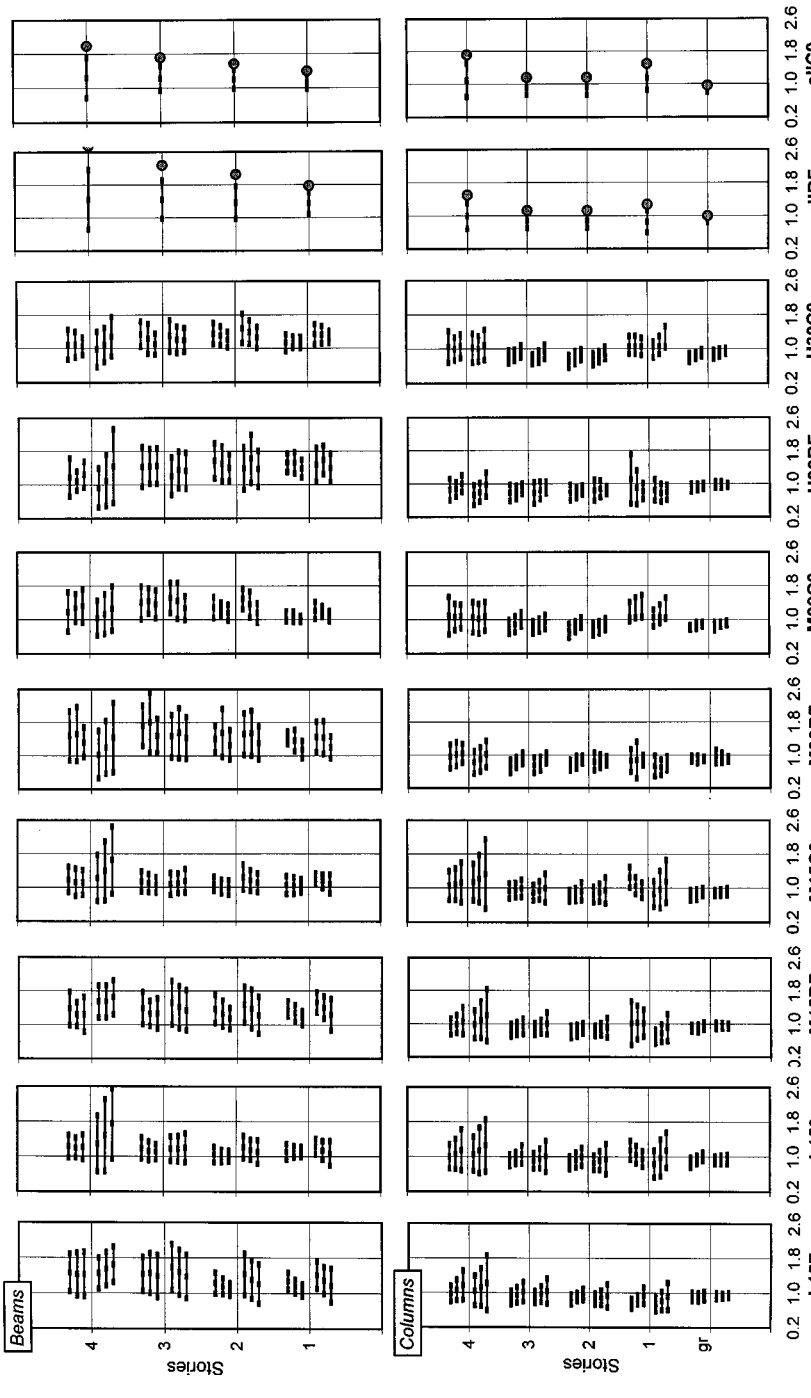

Figure 7. Mean ± standard deviation range of inelastic-to-elastic ratio of chord rotations in individual four-storey buildings, with either 'full' (F) or 'zero' (0) slab participation to beam tension flange and with conventional (C) or relaxed (R) column capacity design. (Upper three or lower three ranges: X or Y direction. Top or bottom range in the triplet: design motion x2 or x1; intermediate: x1·5)

deformation demands is smaller there. The overall mean and the average upper characteristic value are about 1·0 and 1·5, respectively.

Representative examples of the more detailed variation of the results within a single building type are presented in Figure 6 for the interstorey drifts and Figure 7 for chord rotations. Both figures refer to the four-storey structures and to multimodal response spectrum elastic analysis. They present separately the results for versions C0 (conventional capacity design and 'zero' slab contribution to the beams) and RF (relaxed capacity design and 'full' slab contribution to beams) of buildings L15, M15, M30 and H30. Six $m \pm \sigma$ ranges are shown at each floor level instead of the one in Figures 4 and 5: the top three refer to horizontal direction X and the three at the bottom to Y. The bottom one of the three ranges refers to motion intensity 1·0x, the top to 2·0x and the middle one to 1·5x. The scatter in the individual plots in Figure 6 reflects only variability due to the input motion (cf. the coefficient of variation of 7·5 per cent computed in Section 3.1 for the scatter of the individual spectral values with respect to the target spectrum), whereas that in the individual plots of Figure 7 reflects mainly member-to-member variability, which is essentially model uncertainty. It is clear from these two figures that there is no systematic effect of motion intensity, horizontal direction, or seismic design parameters (L15 v. M15, etc.) on the results. Figure 7 shows a small but persistent effect of the beam-to-column strength ratio, as reflected in the extreme cases C0 and RF, but is opposite to what is expected. Cases C0 with the low beam–column strength ratio have lower inelastic-to-elastic chord rotation ratios in the beams, in comparison to cases RF which have higher beam–column strength ratio. The opposite is observed in the columns. It seems that the elastic analysis tends to overpredict, on the basis of member stiffnesses, any concentration of inelasticity to the beams.

To give an idea of the order of magnitude of the deformation demands encountered in the computed non-linear response, Figure 8 presents the (average for the four input motions) interstorey drift ratios of the three DC H buildings subjected to an intensity of 2x the design motion. These are the cases with the largest deformation demands. The building versions shown in Figure 8 correspond to full capacity design and full slab width (cases C and F). To get an idea of the member inelasticity implied by the values in Figure 8, it should be kept in mind that interstorey drift ratios are equal to the sum of the average chord rotation in the beams and the columns of the storey and that chord rotations at yield for RC frame members (including the effect of bar slippage in the joints) range from 0·5 per cent to 1·5 per cent. It is noteworthy that the maximum discrepancy between elastic and inelastic chord rotation demands (Figures 4 and 5) occurs where these demands are the lowest, i.e. in the upper storeys.

3.5. Inelastic deformation demands in open-ground-storey infilled structures

In (partially) infilled RC structures with the ground storey open, inelastic deformation demands tend to concentrate in the open storey. At excitations above the design ground motion the predominant period of the response of the open-ground-storey structure approaches the fundamental period of the elastic structure with the secant-to-yield stiffness of its members. Even though the infills above the ground storey separate from the frame at such ground motion intensities, they are quite effective in limiting the interstorey drift ratios of the infilled storeys. Often the column and the beam chord rotations in these storeys have opposite signs (meaning that bending of the columns in infilled storeys takes place in the opposite sense with respect to the ground storey), so that their algebraic sum is consistent with a storey interstorey drift ratio close to zero.[27,32]

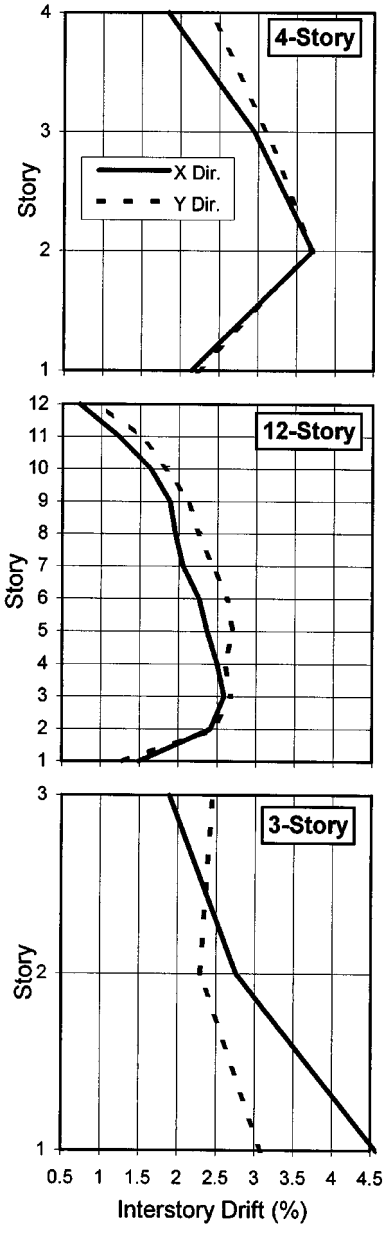

Figure 8. Computed inelastic interstorey drift ratios for DCH buildings designed with full capacity design and full slab width (average for four motions at twice the design intensity)

On the basis of these observations, the elastic model proposed herein for the estimation of inelastic member deformation demands in open-ground-storey RC structures assumes that the elastic rigidity EI of all RC members is the secant-to-yielding in antisymmetric bending, $EI = (M_y/\theta_y)L/6$, and considers the infills as rigid bidiagonal struts in the corresponding bays of the frame. An attractive feature of such a model is that it does not require knowledge of *in-situ* strength or stiffness properties of the masonry and of the infill panels (for new structures such properties are difficult to estimate *a-priori* during design or to control during construction, while for existing structures they are hard to quantify through *in-situ* testing). The effect of the overestimation of infill stiffness in the model is at least partly compensated by the use of the secant-to-yield as the effective elastic rigidity of RC members. The assumption of rigid infills and elastic frame with secant-to-yield EI-value captures well the predominant period of the non-linear response and the drift and member deformation demands in the open ground storey. The accuracy of this model for the member inelastic deformation demands in the infilled storeys is not of much interest, as these members remain essentially elastic and any damage to them is more likely to be due to local effects of the infills than to their own chord rotations demands.

For the rigid-infill elastic model and with the focus on the ground-storey deformations, higher mode effects are not of interest and an equivalent static elastic analysis under lateral loads with an inverted triangular distribution suffices. The ratio of inelastic chord rotation demands in the open-storey members to the corresponding chord rotations from the proposed elastic model and analysis procedure are presented in Figure 9. No significant effect of the seismic design parameters (L15, M15, M30 or H30) or of the horizontal direction were detected in the results, so their influence is lumped together with that of the input excitation (the four synthetic motions) and of the member-to-member variability, into the mean $\pm$ standard deviation ranges, etc., of Figure 9. However, the effect motion intensity is considered worth showing separately, as often the inelastic-to-elastic chord-rotation ratio at 2x the design motion intensity (the top among the two ranges shown) is higher than at 1x the design motion (the bottom one of the two ranges) for the open-storey columns and lower for the open-storey beams. Another factor with a significant effect is the design and not the open-storey elements for a concentration of demands in that storey. Upgrading the resistance of the beams of the first floor (Figure 9(b)) or of the columns of the ground storey (Figure 9(b) and 9(c)) against such a concentration of demands, reduces the inelastic chord rotation in the upgraded elements relative to the elastic ones predicted by the proposed model.

Despite the fact that it represents the Eurocode 8, Part 1–3 approach, case (b) of Figure 9 is not expected to be encountered often in practice. Case (a) is representative of existing buildings, in which the presence of infills above the ground storey has been neglected in the design of the open-storey elements. Case (c), on the other hand, can be considered close to new buildings in which the designer takes reasonable measures to protect the open ground storey from unacceptable concentration of damage. Table IV summarizes the results of Figure 9(a) and 9(c), after eliminating the effect of motion intensity.

It is worth mentioning that, even at a motion intensity of 2x, the interstorey drift ratio in the open ground storey is, on the average for the three cases (a)–(c), about the same as in the bare structure with RC elements proportioned as in case (a).[27,32] It is reminded, though, that this drift ratio is equal to the sum of the average chord rotations of the columns and beams of the ground storey. As in the open ground storey the beam chord rotations are very small, for approximately the same interstorey drift ratio chord rotation demands in the open-storey columns are significantly larger than in the bare structure.

Table IV. Inelastic-to-elastic chord rotation ratio in open-ground-storey elements (mean and 95 per cent-characteristic value)

No. of storeys	Beams		Columns							
			Not-proportioned for open-storey effect				Proportioned for open-storey effect			
			Bottom		Top		Bottom		Top	
	Mean	95 percent-characteristic	Mean	95 per cent-characteristic	Mean	95 per cent-characteristic	Mean	95 per cent-characteristic	Mean	95 per cent-characteristic
4	0.65	0.9	0.95	1.3	1.2	1.75	0.65	0.8	0.55	0.9
12	0.8	1.1	0.85	1.0	1.15	1.85	0.7	0.95	1.1	1.85
3	0.65	1.0	1.0	1.35	1.25	1.75	0.7	0.95	0.8	1.3
All	0.7	1.0	0.95	1.2	1.2	1.8	0.7	0.9	0.8	1.35

The other extreme case of an elastic analysis which is independent of the exact properties of the infills is one in which the infills above the ground storey are neglected and the structure is considered as bare. The fundamental period and, with it, the spectral displacement representative of the equivalent SDOF system increase in such a model, compared to those resulting from the elastic model with rigid infills. However, this larger global displacement is distributed to the other storeys more uniformly and deformations in the ground storey are underestimated. Detailed results exhibit larger scatter and are on the average higher than those of Figure 9. Final conversion factors, to be compared with those at the bottom line in Table IV, are closer to 1·0 for the mean but significantly exceed 1·0 for the upper-characteristic value.

4. CONCLUSIONS

A simple linear-elastic analysis procedure has been developed for the estimation of the mean and 95 per cent-characteristic values of inelastic chord rotation demands in the individual members of multistorey RC frame buildings. For bare structures a multimodal response spectrum elastic analysis should preferably be used, although an equivalent static analysis under lateral loads with an inverted triangular distribution is acceptable. For partially infilled structures with the ground storey open, the infills should be included in the elastic model as rigid bidiagonal struts. In both cases the 5 per cent-elastic spectrum is employed and the elastic rigidities of RC members are taken equal to their secant stiffness at yielding of both ends in antisymmetric bending, i.e. as $EI = (M_y/\theta_y)L/6$. Conversion factors listed at the bottom of Tables III and IV can be used to convert elastic chord rotation demands to mean or 95 per cent-characteristic values of inelastic chord rotations (see Figure 9). For bare structures linear interpolation between the conversion factors for the base and the roof levels of the building can be applied. Conversion factors for the mean value are around 1·0, while those for the upper-characteristic values are around 1·3 at the base (including open ground storeys) and increase in bare structures to values around 1·75 at the top, with a heightwise average value of about 1·5.

The present proposal is essentially a generalization and elaboration of the well-known equal-displacement rule of SDOF systems. Its success herein is due to the fact that the fundamental period of the cracked elastic structures considered is indeed beyond the 'corner' or 'predominant' period T_c of the input motion. As the vast majority of RC frame buildings are expected to have, after extensive cracking, fundamental periods above the 'predominant' one of the ground motion, the present conclusions can be extended to the entire class of ordinary RC buildings, existing or new. So these conclusions can be applied either for displacement-based design of new, or for the displacement-based assessment of existing buildings.

Although it has been developed on the basis of non-linear analyses of frame structures which are completely regular and symmetric in plan and (with one exception out of three) very regular in elevation as well, the proposed procedure with the multimodal response spectrum analysis in 3D is expected to be applicable to structures which are fairly irregular in elevation and/or in plan, at least to the same extent as multimodal response spectrum analysis in 3D is considered applicable for such structures for calculation of seismic internal forces for proportioning purposes. This is an advantage of the proposed procedure over other alternatives based in part on a non-linear static (pushover) analysis, as this latter—unfamiliar to most practitioners—analysis procedure does not account for higher mode effects and its extension to torsionally unbalanced structures has only recently been attempted. The generality of the proposed procedure is also an advantage over

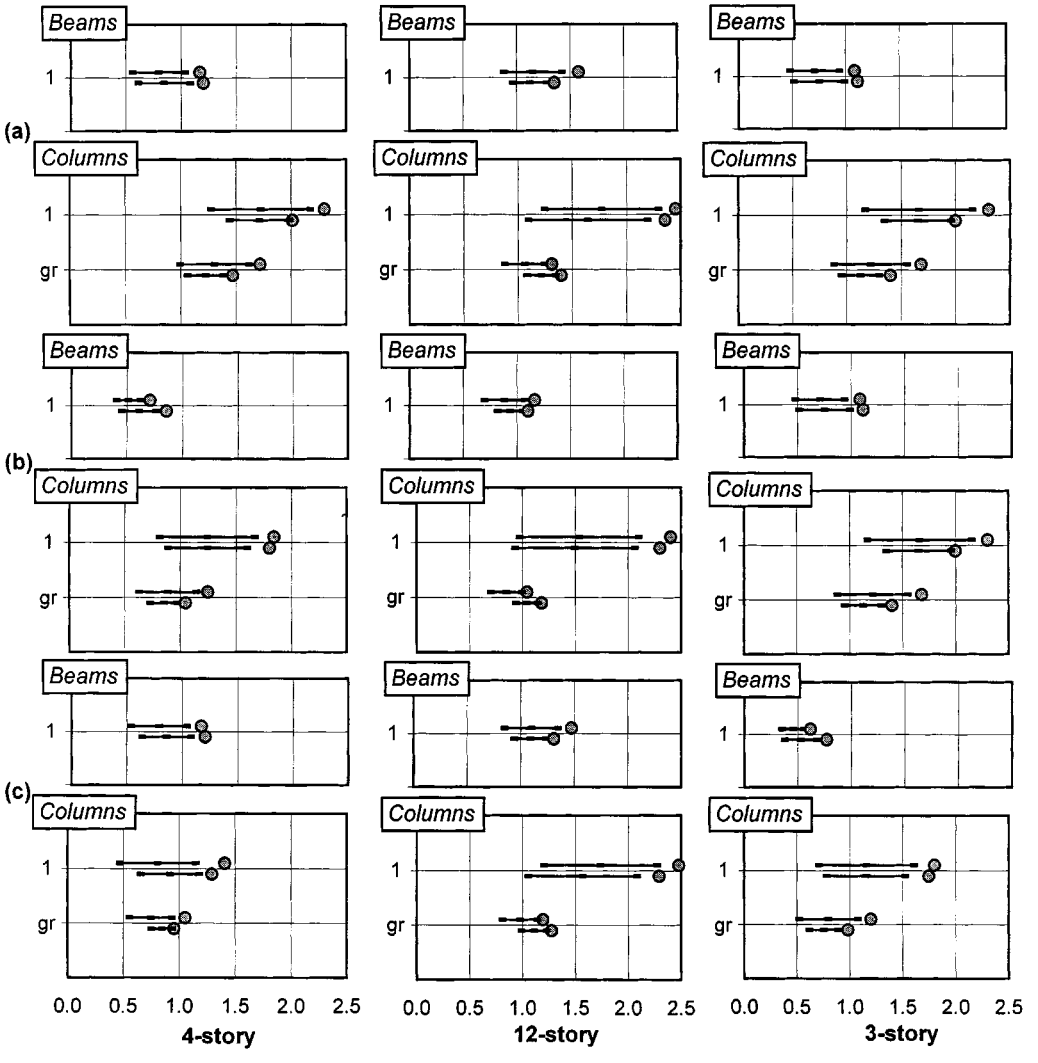

Figure 9. Mean ± standard deviation range and 95 per cent-characteristic value of inelastic-to-elastic chord rotation ratio in open storey of partially infilled buildings: with (a) open-storey members designed as in bare frame; (b) open-storey beams and columns designed against soft-storey effect according to EC8; (c) open-storey columns designed for soft-storey effect according to EC8

other alternatives which, at certain stages, employ conversion factors empirically fitted to the analyses of specific structural configurations. (Herein the conversion factor for the mean value is essentially 1.0, while that for the upper characteristic is for—mainly model—uncertainties which are not covered by alternative procedures.) A final advantage of the proposed procedure is that it goes directly to member chord rotations, which are a most meaningful deformation measure for the assessment or proportioning of RC members. The most serious disadvantage of the proposed

procedure, namely its dependence on *a-priori* knowledge or estimation of member longitudinal reinforcement, is only apparent, as it is commonplace now that it is impossible to estimate with some degree of accuracy displacement and deformation demands in RC structures on the basis of cross-sectional dimensions alone, without some knowledge of the amount and distribution of the longitudinal reinforcement.

ACKNOWLEDGEMENTS

This work was supported by Directorate General XII of the European Commission, under contract No. ENV4-CT97-0548 (DG 12 - ESCY) of its 'Environment' program ('NODISASTR' project) and contract No. FMRX-CT96-0022 (DG12-RSRF) of its TMR (Training and Mobility of Researchers) program ('ICONS' Research Network).

REFERENCES

1. X. Qi and J. P. Moelhe, 'Displacement design approach for reinforced concrete structures subjected to earthquakes', *EERC Report No. UCB/EERC-91/02*, Earthquake Engineering Research Center, University of California at Berkeley, CA, 1991.
2. J. P. Moehle, 'Displacement-based design of R/C structures subjected to earthquakes', *Earthquake Spectra* **8**(3), 403–428 (1992).
3. M. J. N. Priestley, 'Myths and fallacies in earthquake engineering—conflicts between design and reality', *Proc. T. Paulay Symp. Recent Developments in Lateral Force Transfer in Buildings*, La Jolla, California, 1993.
4. J. W. Wallace, 'New methodology for seismic design of R/C shear walls', *J. Struct. Engng.* ASCE, **120**(3), 863–884 (1994).
5. G. M. Calvi and G. R. Kingsley, 'Displacement based seismic design of multi-degree-of-freedom bridge structures', *Earthquake Engng. Struct. Dyn.* **24**, 1247–1266 (1995).
6. M. J. N. Priestley, 'Displacement-based approaches to rational limit states design of new structures', Closing Lecture, *11th European Earthquake Engineering Conf.*, Paris, 1998.
7. M. N. Fardis and T. B. Panagiotakos, 'Displacement-based design of RC buildings', in P. Fajfar and H. Krawinkler (eds), *Seismic Design Methodologies for the Next Generation of Codes*, Balkema, Rotterdam, 1997, pp. 195–206.
8. T. B. Panagiotakos and M. N. Fardis, 'Deformation-controlled seismic design of RC structures', *11th European Conf. Earthquake Engineering*, Paris, 1998.
9. M. J. N. Priestley, 'Displacement-based seismic assessment of reinforced concrete buildings', *J. Earthquake Engng*, **1**(1), 157–192 (1997).
10. M. N. Fardis, 'Seismic assessment and retrofit of RC structures', *11th European Conf. Earthquake Engineering*, Paris, 1998.
11. Applied Technology Council, 'NEHRP Guidelines for the seismic rehabilitation of buildings', *FEMA Report No.* 273, Washington, DC, 1997.
12. E. Miranda, 'Evaluation of site-dependent inelastic seismic design spectra', *J. Struct. Engng.* ASCE, **119**(5), 1319–1338 (1993).
13. E. Miranda, 'Site-dependent strength reduction factors', *J. Struct. Engng.* ASCE, **119**(12), 3505–3519 (1993).
14. N. Lam, J. Wilson and G. Hutchinson, 'The ductility factor in the seismic design of buildings', *Earthquake Engng. Struct. Dyn.* **27**, 749–769 (1998).
15. J. Alonso, E. Miranda and P. Santa-Ana, 'Inelastic displacement demands for structures built on soft soils', *Proc. 11th World Conf. on Earthquake Engineering*, Paper No. 40, Acapulco, 1996.
16. G. D. P. K. Seneviratna and H. Krawinkler, 'Modifications of seismic demands for MDOF systems', *Proc. 11th World Conf. on Earthquake Engineering*, Paper No. 2129, Acapulco, 1996.
17. E. Miranda, 'Estimation of maximum interstorey drift demands in displacement-based design', in P. Fajfar and H. Krawinkler (eds), *Proc. Workshop on 'Seismic Design Methodologies for the Next Generation of Codes'*, Balkema, Rotterdam, 1997, pp. 253–264.
18. Applied Technology Council, 'Seismic evaluation and retrofit of concrete buildings', *Report No. ATC-40*, Redwood City, CA, 1996.
19. Comite Europeen de Normalisation, European Pre-standard ENV 1998-1–3: 'Eurocode 8—Design provisions for earthquake resistance of structures—Part 1–3: General rules—Specific rules for various materials and elements', Bruxelles, November, 1994.

20. T. B. Panagiotakos and M. N. Fardis, 'Effect of column capacity design on earthquake response of reinforced concrete buildings', *J. Earthquake Engng*, **2**(1), 113–145 (1998).
21. T. B. Panagiotakos, 'Displacement-based seismic design of RC buildings', *Doctoral Thesis*, Department of Civil Engineering, University of Patras, Patras (in Greek), 1998.
22. Y. J. Park and A. M. S. Ang, 'Mechanistic seismic damage model of reinforced concrete', *J. Struct. Engng.* ASCE, **111**(4), 722–739 (1985).
23. Y. J. Park, A. M. S. Ang and Y. K. Wen, 'Damage-limiting aseismic design of buildings', *Earthquake Spectra* **3**(1), 1–26 (1987).
24. S. Otani, 'Inelastic analysis of R/C frame structures', *J. Struct. Div. ASCE* **100**(ST7), 1433–1449 (1974).
25. R. J. Mainstone, 'On the stiffnesses and strengths of infilled frames', *Proc. Inst. Civil Engrs.* iv, 7360s (1971).
26. M. N. Fardis and T. B. Panagiotakos, 'Hysteretic damping of reinforced concrete elements', *Proc. 11th World Conf. on Earthquake Engineering*, 1996, Paper P-5(464), Acapulco.
27. M. N. Fardis, (Ed.) 'Experimental and numerical investigation on the seismic response of RC infilled frames and recommendations for code provisions', *ECOEST/PREC8 Report No. 6*, Laboratorio Nacional de Engenharia Civil, Lisbon, 199p., 1996.
28. A. K. Chopra, *Dynamics of Structures*, Prentice-Hall, New York, 1995.
29. M. N. Fardis and T. B. Panagiotakos, 'Seismic design and response of bare and masonry-infilled reinforced concrete buildings. Part I: Bare structures', *J. Earthquake Engng.* **1**(1), 219–256 (1997).
30. M. N. Fardis, S. N. Bousias, G. Franchioni and T. B. Panagiotakos, 'Seismic response and design of RC structures with plan-eccentric masonry infills', *Earthquake Engng. Struct. Dyn.*, 1999, to appear.
31. S. N. Economou, M. N. Fardis and A. Harisis, 'Linear elastic v non-linear dynamic seismic response analysis of RC buildings', in Moan et al. (eds.), EURODYN '93, 2*nd European Conf. on Structural Dynamics*, *Trondheim*, Balkema, Rotterdam, pp. 1993, 63–70.
32. M. N. Fardis and T. B. Panagiotakos, 'Seismic design and response of bare and masonry-infilled reinforced concrete buildings. Part II: Infilled structures', *J. Earthquake Engng.* **1**(3), 475–504 (1997).

